frontiers in Integrative Neuroscience

ORIGINAL RESEARCH
published: 10 August 2020
doi: 10.3389/fnint.2020.00043

Antero-Posterior vs. Lateral Vestibular Input Processing in Human Visual Cortex

Felipe Aedo-Jury[1,2], *Benoit R. Cottereau*[1,2], *Simona Celebrini*[1,2] *and Alexandra Séverac Cauquil*[1,2]*

[1]*Centre de Recherche Cerveau et Cognition, Université Touloue III Paul Sabatier, Toulouse, France,* [2]*Centre National de la Recherche Scientifique, Toulouse, France*

Visuo-vestibular integration is crucial for locomotion, yet the cortical mechanisms involved remain poorly understood. We combined binaural monopolar galvanic vestibular stimulation (GVS) and functional magnetic resonance imaging (fMRI) to characterize the cortical networks activated during antero-posterior and lateral stimulations in humans. We focused on functional areas that selectively respond to egomotion-consistent optic flow patterns: the human middle temporal complex (hMT+), V6, the ventral intraparietal (VIP) area, the cingulate sulcus visual (CSv) area and the posterior insular cortex (PIC). Areas hMT+, CSv, and PIC were equivalently responsive during lateral and antero-posterior GVS while areas VIP and V6 were highly activated during antero-posterior GVS, but remained silent during lateral GVS. Using psychophysiological interaction (PPI) analyses, we confirmed that a cortical network including areas V6 and VIP is engaged during antero-posterior GVS. Our results suggest that V6 and VIP play a specific role in processing multisensory signals specific to locomotion during navigation.

Keywords: fMRI, galvanic vestibular stimulation (GVS), visual cortex, V6, VIP, visuo-vestibular integration

OPEN ACCESS

Edited by:
Christophe Lopez, Centre National de la Recherche Scientifique (CNRS), France

Reviewed by:
Mark W. Greenlee, University of Regensburg, Germany
Sebastian Martin Frank, Brown University, United States
Yong Gu, Institute of Neuroscience, Shanghai Institutes for Biological Sciences, Chinese Academy of Sciences, China

***Correspondence:**
Alexandra Séverac Cauquil
alexandra.severac@cnrs.fr

Received: *28 January 2019*
Accepted: *10 July 2020*
Published: *10 August 2020*

Citation:
Aedo-Jury F, Cottereau BR, Celebrini S and Séverac Cauquil A (2020) Antero-Posterior vs. Lateral Vestibular Input Processing in Human Visual Cortex. Front. Integr. Neurosci. 14:43. doi: 10.3389/fnint.2020.00043

INTRODUCTION

Self-motion (egomotion) perception permits us to estimate our on-going change of position within the surrounding space to properly interact with our environment. In the brain, egomotion is processed from multisensory inputs, particularly vestibular and visual ones whose integration remains poorly understood (e.g., Britten, 2008).

In macaques, several groups have shown vestibular projections in the medial superior temporal area (MST), a visual area involved in object-motion and self-motion perception based on optic flow (Duffy, 1998; Bremmer et al., 1999; Gu et al., 2006). MST projects towards the ventral intraparietal area (VIP) that is sensitive to visual heading and receives vestibular inputs (Klam and Graf, 2003a,b). A recent study demonstrated that the visual posterior area (VPS), located at the posterior end of the Sylvian fissure, also contains multi-sensory neurons that process both optic flow and vestibular signals (Chen et al., 2011).

In humans, neuroimaging studies revealed several brain regions involved in visual egomotion processing. For example, Wall and Smith (2008) found that the ventral intraparietal (VIP) and the cingulate sulcus visual (CSv) areas had selective responses to optic flow patterns that are compatible with those received by our retina during locomotion (i.e., a selectivity to egomotion-consistent

optic flows). A preference for egomotion-consistent visual pattern, although weaker, was also reported in human MST (Morrone et al., 2000). Human MST might, therefore, constitute an intermediate stage of egomotion processing which is further developed in areas VIP and CSv. A follow-up study (Cardin and Smith, 2010) used wide-field visual stimuli to demonstrate that putative area V6 and two vestibular areas, the parieto-insular vestibular cortex (PIVC) and putative area 2v, in the postcentral sulcus (p2v) were also included in a network processing egomotion. As the natural stimulus for the vestibular apparatus, head motion, is incompatible with functional neuroimaging constraints, artificial vestibular stimulation is needed. Both caloric and galvanic stimulations are the two main methods used in functional magnetic resonance imaging (fMRI) designs (see Lopez et al., 2012). Galvanic vestibular stimulation (GVS) presents the advantage of providing stimulation that: (1) involves all vestibular afferents (Fitzpatrick and Day, 2004) as it has been recently evidenced on behaving primates (Kwan et al., 2019); and (2) may be orientated differently according to electrodes position and polarisation (Séverac Cauquil et al., 2000; Aoyama et al., 2015). Using GVS, Smith et al. (2012, see also Billington and Smith, 2015) showed that MST and CSv were also vestibularly-driven, which strengthen their role in egomotion processing. In the same study, responses to GVS in V6 and VIP were very weak if not absent. However, these authors used the classical binaural bipolar configuration where the anode is placed on one mastoid and the cathode on the other. In this case, GVS is known to elicit a lateral postural tilt towards the anode when the body is free to move (e.g., Njiokiktjien and Folkerts, 1971; Nashner and Wolfson, 1974; Lund and Broberg, 1983), but also a feeling of motion in the opposite, yet lateral, direction (Fitzpatrick et al., 2002; Fitzpatrick and Day, 2004). These responses are compatible with an activation of the parts of the vestibular apparatus sensitive to roll tilt, in the frontal plane (Séverac Cauquil et al., 2003; Day et al., 1997). Therefore, such a GVS design prohibits the investigation of the contribution of the antero-posterior motion signal. Yet, human motion, in particular locomotion, mostly refers to forward displacements: it principally includes translational egomotion in the postero-anterior (i.e., forward) direction. If walking and running involve a complex pattern of acceleration and deceleration that also comprises vertical translation and sagittal rotation, these components are nevertheless minimized to stabilize the head (Pozzo et al., 1990). The cortical networks engaged in visuo-vestibular integration during antero-posterior egomotion might, therefore, be different from those involved during lateral egomotion. The different pathways followed for motion-in-depth processing compared to lateral motion, V3A, and hMT+ being specifically involved in the former, processing supports this hypothesis (Cottereau et al., 2014). So does the finding that different areas such as MST and V6 would encompass dissociated components of self-motion from optic flows, i.e., heading for the former and obstacle avoiding for the latter (Cardin et al., 2012a).

In the present study, we (1) reproduced Smith et al.'s (2012) paradigm using different stimulation parameters to determine whether the set of visual areas that they found can be reliably activated by a different type of lateral GVS. We also (2) determined whether antero-posterior vestibular inputs activated a different cortical network. In that aim, we used binaural monopolar GVS, since this design (although much less common) has been shown to induce a body response and self-motion illusion in the antero-posterior plane (Séverac Cauquil et al., 1998, 2000; Magnusson et al., 1990; Aoyama et al., 2015): forward when anodes are on the forehead and backward with anodes over the mastoid processes. Such postural tilts in the antero-posterior direction fit with the model proposed by Day et al. (2011). They postulate that by polarizing equally both vestibular apparatus, binaural monopolar GVS provides a fake backward or forward self-motion input. Among several studies indicating that GVS induces a postural tilt towards the anodes, counteracting the action direction (away from the anodes), the most recent demonstrated the perfect adequacy between subjective perceptual responses and objectively quantified head movements, for both lateral and antero-posterior GVS stimulations (Aoyama et al., 2015). Here, we combine this tool with fMRI to differentiate the visual cortical networks activated during antero-posterior (AP) and lateral (L) GVS.

MATERIALS AND METHODS

Participants

Thirteen healthy human subjects (mean age 28.4, range 19–45, seven females) were included in this study. Eleven were right-handed, as assessed with the Edinburgh Inventory (Oldfield, 1971). They all participated in the galvanic stimulation experiment. Eleven of them also performed an additional experiment that included functional localizers. All subjects had normal or corrected-to-normal vision reported no history of neurological or psychiatric disease, and gave written informed consent before participation, following the Declaration of Helsinki. This study was approved by the local ethics committee (ID RCB: 2012-A01052-41). Subjects received 80 euros of monetary compensation for their participation.

Stimuli and Design

Galvanic Stimulation

Vestibular stimuli consisting of 2 s of 1 mA square-pulses were delivered by two identical dedicated current-limited stimulators [DS5, Digitimer, UK, CE certified for biomedical research N(IEC) 60601] through four disposable carbon electrodes (Skintact, FSWB00) placed on the forehead and over the mastoid processes (see **Figure 1**).

The stimulators were localized outside the scanner room and were connected to screen cables through a waveguide. Four GVS configurations were used. Two bilateral monopolar configurations with anodes over the mastoids (**Figure 1A**, top) or the forehead (**Figure 1A**, bottom), respectively permitted to elicit vestibular activations consistent with a forward or backward motion of the body (antero-posterior GVS). Two bilateral bipolar conditions with anode right/cathode left (**Figure 1B**, top) or cathode right/anode left (**Figure 1B**, bottom) permitted to evoke activations consistent with leftward or rightward motion (lateral

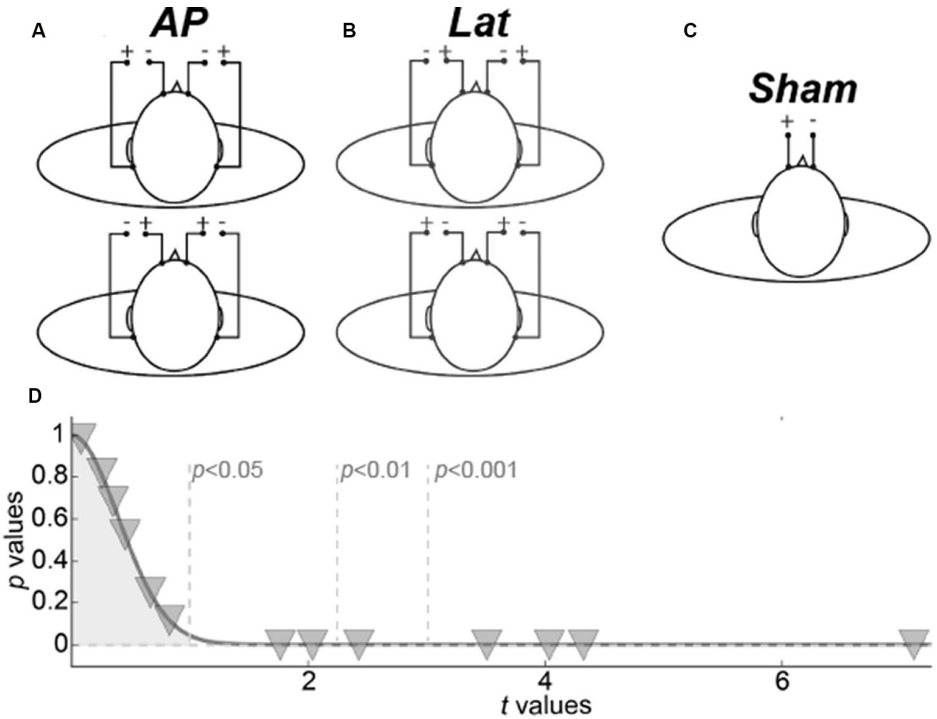

FIGURE 1 | Galvanic vestibular stimulation (GVS) procedure. **(A)** The two antero-posterior configurations. **(B)** The two lateral configurations. **(C)** Sham configuration. **(D)** Representation of behavioral results. Inverted triangles give the *p*- and *t*-values of the permutation tests for each subject.

GVS). The amplitude of the postural reaction is known to vary with GVS intensity until reaching a plateau (Séverac Cauquil et al., 1998). For that reason, on top of obvious avoidance of tactile or even painful stimulation, we chose to use low, 1 mA, GVS intensity. Therefore, because the subjects were not always aware of the stimulation, a beep sound informed them every time a stimulation was delivered. As a baseline, we used a no-GVS condition that started with a beep but without any stimulation. Data were collected using an event-related design within which runs lasted 5 min (300 s) and comprised 40 events (eight for each of our five conditions). The time interval between the two condition onsets was fixed to 7.5 s. Behavioral responses were recorded during the scans: subjects were instructed to perform a forced-choice task using a 4-button box. After each beep, they had to press either the left or the right button to report whether they had experienced a sensation of self-motion along the lateral axis (L) or either the up or the down button in case of antero-posterior, AP, self-motion. The statistical significance of these L vs. AP responses were evaluated for each subject through permutations tests (**Figure 1D**). For these permutation tests, we computed 10,000 synthetic means by randomly subsampling 27 trials from the 54 of the sham condition. We generated representative distributions of these mean values. A *z*-score and its corresponding *p*-value were then obtained by dividing the observed mean for the subjects in the stimulation trials by the standard deviation of the Gaussian distribution generated by the permutation tests (and always centered on ∼1).

To control that our fMRI results were caused by vestibular activations rather than by somatosensory effects induced by the galvanic stimulation, we also designed a sham condition during which the same stimulation (i.e., a 2 s square pulse of 1 mA) was only delivered between the two frontal electrodes (**Figure 1C**). Responses to these stimulations were recorded during a separated run of 5 min that comprised 40 events whose onsets were separated by 7.5 s. The GVS and sham runs were conducted in total darkness on subjects instructed to keep their eyes closed during the whole recording to avoid any visual stimulation. We discuss the possible implications of eye movements on our results in the "Control for Vergence" section.

Localizers for Areas Responding to Egomotion-Compatible Optic Flow

In this study, our main analyses were performed within functionally defined Regions of Interest (ROIs) that preferentially respond to egomotion compatible optic flow. This ROI-based approach enables us to directly compare ROI data across subjects. It also gets rid of the multiple comparisons problem because statistics are only performed within the predefined ROIs (see e.g., Poldrack, 2007). To localize the cortical areas that respond to egomotion-compatible optic flow, we used the stimuli described in previous studies (see e.g., Wall and Smith, 2008; Cardin and Smith, 2010). It consisted of 500 moving white dots displayed at 60 Hz on a black background and arranged in an egomotion-consistent (EC) or egomotion-inconsistent (EI) optic flow pattern. In the EC condition, the

optic flow pattern had both expansion/contraction and rotation components that varied over time, consistent with self-motion on a varying spiral trajectory (Morrone et al., 2000). The EI stimulus consisted of a 3 × 3 array of nine identical panels, each containing a smaller version of the EC stimulus. Although the individual panels contained optic flow, the overall pattern was not consistent with egomotion because flow induced by observer motion can have only one center of motion. Stimuli were presented using a block-design. Runs consisted of 224 s (3 min, 44 s) divided into seven identical cycles of 32 s. In half of the runs, a cycle started with a baseline of 10 s where only the fixation point was present. It was followed by 6 s of the EC condition, then by another 10 s of blank and finally by 6 s of the EI condition. In the other half of the runs, the EC and EI conditions were inverted within a cycle (i.e., a cycle had 10 s of blank, 6 s of the EI condition, 10 s of blank, and finally 6 s of the EC condition). During the recordings, subjects were instructed to passively keep their eye on the central fixation point. They, however, all reported that the EC conditions elicited a strong percept of egomotion.

The localizers for the ROI responding to egomotion-compatible optic flow were presented via an LCD projector, back-projected onto a screen positioned at the end of the scanner bore, and viewed through a mirror mounted on the head coil. The viewing distance was 130 cm. It led to squared stimuli of 16°×16°.

Data Acquisition

All the data were collected on a 3T scanner (Philips Achieva), using a standard 32 channels head coil. The functional data were acquired using (T2*-weighted) echoplanar imaging (EPI). The data for the main experiment (GVS) were collected during the first session. The data for the functional localizers were collected during a second session.

For the GVS experiment, we used the following prescription that is quite generic for whole-brain recordings: repetition time (TR) = 2.5 s, echo time (TE) = 30 ms, voxel size 3 × 3 × 3 mm, no gap thickness, flip angle (FA) = 77°, SENSE factor = 2.8. Each run comprised 120 volumes of 41 transversally oriented slices that covered the whole brain. In total, we collected 10 runs (eight runs with the four main conditions and the baseline and two additional runs with the sham stimulations, see the "Galvanic Stimulation" section above). The total duration of the recordings was about 45 min.

For the functional localizers, because the cortical regions that selectively respond to egomotion consistent optic flow are now well established in the occipital and parietal regions (see e.g., Cardin and Smith, 2010 or Smith et al., 2012), we used a prescription specifically designed to optimize the resolution of BOLD recordings in these particular regions: TR: 2 s; TE: 30 ms; the field of view (FOV): 210 mm; voxel size 2 × 2 × 2 mm; no gap thickness, SENSE factor: 2.5. A run comprised 96 volumes of 33 slices that covered occipital and parietal cortices. We recorded four runs in total (two for each condition).

Both the two sessions of recordings also included the acquisition of a high-resolution anatomic image using a T1-weighted magnetization-prepared rapid gradient-echo (MPRAGE) sequence (160 slices; TR: 2,300 ms; TE: 3.93 ms; FA: 12°; FOV: 256 mm; voxel size 1 × 1 × 1 mm). These anatomical images were first co-registered and then averaged together to be used as a reference to which the functional images from all the experiments were aligned.

Data Analyses

Pre-processing

All the fMRI data were analyzed using the Brain Voyager QX software (v2.8, Brain Innovation) and Matlab. Pre-processing included slice scan time correction, 3D motion correction using trilinear/sinc interpolation, and high-pass filtering (0.01 Hz). For each subject, functional data were co-registered on the anatomy. Functional and anatomical data were brought into ACPC space using cubic spline interpolation and then transformed into standard Talairach (TAL) space (Talairach and Tournoux, 1988).

Region of Interest (ROI) Definition

For each subject who performed the localizers experiment (n = 11), we determined the areas responding to egomotion compatible optic flow (V6, VIP, CSv, hMT+, and PIC) using the contrast between egomotion-consistent (EC) vs. inconsistent (IC) optic flow conditions (see the "Localizers for Areas Responding to Egomotion-Compatible Optic Flow" section above). Except for area V6 for which we used the adaptive statistical threshold procedure proposed in (Cardin et al., 2012b; see below), our functional areas were defined using a threshold of $p < 0.001$ (uncorrected).

V6 seed was determined as the most significant voxel within the parieto-occipital sulcus (POS) for the EC vs. EI contrast. We then grew a V6 cluster around this seed by reducing the threshold until the point in which the cluster started to expand outside the POS (Cardin et al., 2012b). We defined V6 at this threshold. This approach led to the successful identification of area V6 in 10 out of our 11 subjects who underwent the localizers. Because our V6 ROI was not defined from wide-field retinotopic mapping (see e.g., Pitzalis et al., 2006), we cannot be certain about the exact limit of this ROI. We, therefore, propose a control analysis to determine if this uncertainty impacts our results (see the "Results" section).

Using the same contrast between egomotion-consistent (EC) vs. inconsistent (EI) optic flow, we also defined the VIP area. This was the cortical region in the anterior part of the intraparietal sulcus and close to the intersection with the post-central sulcus that was significantly more activated during the EC condition. This location matches with the one reported in the original study of Bremmer et al. (2002), and is consistent with the definition of VIP described in Smith et al. (2012). Using this definition, we were able to define VIP bilaterally in seven of our subjects. For another three subjects, we localized VIP in one hemisphere but not in the other. Then, for each subject, the data corresponding to an ROI that was found bilaterally was averaged across hemispheres.

With the same approach, we defined area CSv in all our subjects and the human middle temporal complex hMT+ in 10 of our 11 subjects. This region was localized within the ascending branch of the inferior temporal sulcus (ITS; see Kolster et al., 2010) and includes MT, MST, and possibly other few motion regions like the putative fundus of the superior temporal area (pFST). Finally, our contrast also revealed a visually responsive region in the vicinity of the parieto-insular cortex (PIC) in nine of our subjects. This region corresponds to an area originally described by Sunaert et al. (1999), and that responds more strongly to the egomotion-consistent stimuli (see Billington and Smith, 2015). PIC was recently proposed as a putative homolog of macaque VPS (Frank et al., 2014), anatomically and functionally distinct from the PIVC since PIC is activated, and PIVC suppressed by visual stimulation (Frank and Greenlee, 2018). To investigate the differences between these two areas, we included PIVC as a supplementary ROI. Since it was not possible to localize it from our visual localizers, we defined it by using published average coordinates of PIVC (Frank et al., 2016): a sphere of 300 voxels was drawn around the center of Talairach coordinates (−43, −14, 17 and 40, −14, 18 for left and right hemisphere respectively) and the beta values extracted for each subject from the normalized Talairach brain (**Supplementary Figure S2A**).

The average TAL coordinates of these ROIs in all our subjects, provided in **Table 1**, fit very well with those reported in previous studies. **Figure 2A** shows the results of the contrast between egomotion-consistent (EC) vs. inconsistent (EI) optic flow and the resulting ROIs in one typical participant.

General Linear Model (GLM)

All our analyses of the functional data used a general linear model (GLM). The data from each participant were analyzed separately. Time series were processed by fitting a regressor formed by convolving the event time course with a standard hemodynamic response function. As GVS induced micro-movements of the participant's head could potentially bias our results, six regressors taken from the head motion correction were also included as regressors of no interest. The responses to our first and second conditions (i.e., the stimulations that elicited a vestibular activation consistent with a forward or a backward motion) were modeled together to form the responses to antero-posterior (AP) stimulations. The responses to our third and fourth conditions (i.e., the stimulations consistent with a leftward or a rightward motion) were also modeled together to form the responses to lateral (lat) stimulations. Finally, the beta values obtained for these two conditions and the sham stimulation were corrected by subtracting the beta values obtained during the baseline condition. Then, we looked at the results at the individual level. Our analysis focuses on ROIs that were specifically involved in the processing of EC optic flow to check whether they also had specific responses to AP or Lat galvanic stimulations. However, we also completed this approach with a preliminary whole-brain analysis that was performed at the individual level. In this case, activations were first displayed as an overlay of a segmented and inflated or flattened representation of each hemisphere based on the average anatomical scan of each subject. Activation maps were thresholded at $p < 0.001$ (uncorrected). This initial whole-brain analysis aimed to obtain a general overview of our data and thereby to avoid pinhole conclusions (see Hupé, 2015).

TABLE 1 | Region of Interest (ROI) comparison with previous studies. For posterior insular cortex (PIC), we provide the coordinates of the anterior (ant.) and posterior (post.) part of the region as reported by Frank et al. (2016).

Area	Mean Coordinate (TAL)	Reference (TAL)	Study
Left V6	−13, −81, 27	−11, −79, 30	Cardin and Smith (2010)
Right V6	15, −76, 30	14, −77, 30	
Left VIP	−45, −41, 38	−40, −40, 42	Bremmer et al. (2001)
Right VIP	41, −48, 40	38, −44, 46	
Left CSV	−10, −25, 40	−10, −25, 38	Wall and Smith (2008)
Right CSV	11, −26, 41	10, −26, 41	
Left MT+	−44, −62, 5	−39, −62, 5	Cardin and Smith (2010)
Right MT+	43, −62, 3	39, −60, −1	
Left PIC	−40, −21, 21	−40, −31, 21 (ant.) −42, −36, 23 (post.)	Frank et al. (2016)
Right PIC	41, −22, 19	37, −30, 18 (ant.) 58, −34, 17 (post.)	

Connectivity Analyses

To characterize functional connectivity between our ROIs during our two conditions, we performed a psychophysiological interaction (PPI) analysis (Friston et al., 1997). This analysis aims at characterizing task or context-specific changes in the relationship between brain areas (see e.g., O'Reilly et al., 2012 for a review). In our specific case, it permitted to establish those cortical areas that are specifically more connected during the AP and Lat stimulations. PPI can be obtained with a GLM that contains three regressors: the psychological variable (in our case antero-posterior/lateral, coded as +1/−1), the physiological variable (the time-course of a seed region) and the PPI regressor (psychological × physiological regressor). Before computing the interaction term, the psychological and physiological time courses were both expressed in terms of the underlying neural activity. To do so, we first estimated the hemodynamic response function and then used it to deconvolve the activity recorded from the seed ROI (Gitelman et al., 2003). The two time-courses (psychological and physiological) were also included in the GLM as covariates of no interest. This means that the variance explained by the interaction term is only that over and above what is explained by the main effects of task and physiological correlation. We constructed one GLM for each of our ROIs. The seed time-course associated with an ROI first corresponded to the average response of the ROI across its voxels. It was then mean-corrected and z-transformed. The psychological variables were the AP GVS condition vs. baseline on the one hand and the Lat condition vs. baseline on the other hand. The PPI predictor of a given seed region was then tested in each of the remaining network nodes in a multisubject RFX GLM (points 3–5, covering the peak of the BOLD response).

To focus our analysis on the connections within our functionally defined ROIs, we performed a multiregional PPI approach (Cocchi et al., 2014; Schindler and Bartels, 2017). Multiregional PPI is a simple generalization of the PPI approach;

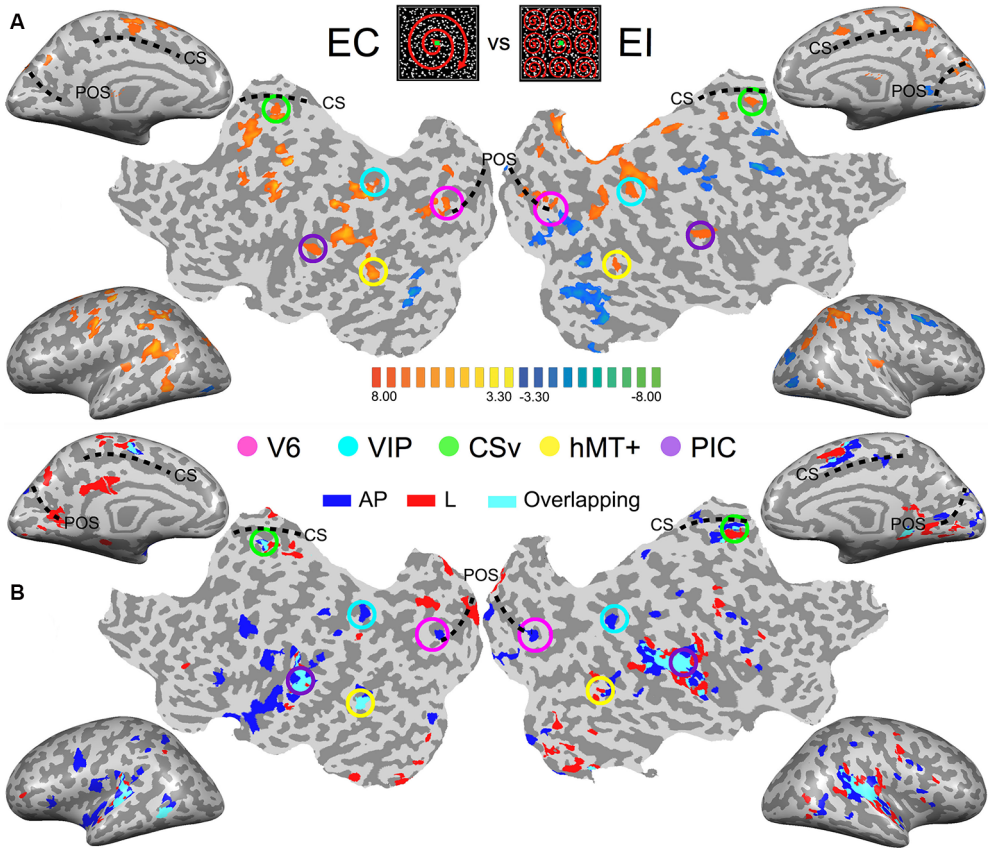

FIGURE 2 | Images from the brain of one participant showing the key results. (Top-center patches) Egomotion-consistent (EC) and egomotion-inconsistent (EI) optic flow patterns used as localizers stimuli. **(A)** Contrast between the cortical responses recorded during the egomotion consistent (EC) vs. inconsistent (EI) optic flow conditions. Data are shown on inflated cortical surfaces and flat maps for the left and right hemispheres ($p < 0.001$, uncorrected). The positions of the parieto-occipital sulcus (POS) and cingulate sulcus (CS) are provided as anatomical landmarks. Colored circles outline the five Regions of Interest (ROIs) in this subject. **(B)** Responses during the galvanic stimulation (GVS) experiment for the same participant. Voxels whose activations were stronger during GVS conditions than during baseline were colored in blue (antero-posterior, AP), red (lateral, lat) and cyan (both) before being superimposed transparently on the inflated brain and flat maps.

it permitted to characterize connectivity between each pair of our functionally defined ROIs (10 pairs in total) rather than between a single-seed region and all the other brain voxels. This analysis was performed at the single-subject level, which helps reduce the uncertainty of the same sample size for PPI analysis. This procedure gives quite robust outcomes since a pair is considered as significant only when it appears as such in the majority of tested subjects. We, therefore, performed nine analyses corresponding to the nine subjects for whom we were able to identify all the ROIs. The PPI predictor of a given ROI was then tested in each of the remaining network nodes in an *ROI-paired* multisubject RFX GLM (points 3–5, covering the peak of the BOLD response).

RESULTS

Behavioral Results

We analyzed the behavioral responses collected for each subject. Although it is well-established that the galvanic stimulation configuration (monopolar vs. bipolar) has a significant effect on the perceived direction of self-motion in standing and lying subjects (Fitzpatrick et al., 2002; Fitzpatrick and Day, 2004; Lepecq et al., 2006; St George et al., 2011; Ferrè et al., 2013; Aoyama et al., 2015), we did not necessarily expect to elicit clear sensations in our experiment because of the short stimulation duration and low intensity used in our design (see the "Galvanic Stimulation" section). At the group-level, we did not find significant differences between the behavioral responses to our AP and Lat conditions (paired t-test $t_{(13)} = 0.16$, $p = 0.87$). Nonetheless, at the individual level, we found that seven of the 13 subjects were able to significantly discriminate between the AP and Lat conditions (**Figure 1D**).

Whole Brain Analysis

As an initial step, we computed for each subject the activation maps during the galvanic stimulation (GVS) conditions using a whole-brain analysis. This enables us to obtain an overview of the data at the individual level and also to compare the

maps across subjects. However, bear in mind that our analysis (at both the individual and the group level) is performed within our functionally defined ROI [see the "General Linear Model (GLM)" section of the "Materials and Methods" and the next section]. For this initial step, we contrasted both the antero-posterior (AP) and lateral (lat) GVS conditions against the baseline. These contrasts for one typical participant are shown in **Figure 2B** ($p < 0.001$, uncorrected). For a direct comparison between visual and vestibular responses, **Figure 2A** also shows a response to optic flow in the same participant.

The responses to lateral GVS (in red) are in good agreement with previous imaging studies that used similar GVS conditions (Bucher et al., 1998; Lobel et al., 1998; Bense et al., 2001). The activity was seen in the PIVC and in putative vestibular areas 2v and 3aNv. Consistently with the previous work of Smith et al. (2012; see their Figure 2), we also found activations in visual areas such as the hMT+ complex or CSv, a portion of the cingulate sulcus that is highly activated during the presentation of egomotion-compatible optic flow—see e.g., Wall and Smith (2008), or Smith et al. (2012). Responses in the other participants were very consistent with those observed here.

Across subjects and hemispheres, responses to antero-posterior GVS stimulation were generally similar to those observed during lateral GVS stimulation. However, the former condition led to stronger responses in several cortical regions. One is located within the posterior part of the POS. Another lies within intra-parietal sulcus, close to its intersection with post-central sulcus. These two regions overlap with our functionally defined ROIs V6 and VIP (see **Figure 2A**, the pink and cyan circles). Outside our visual ROIs, we did not find any region that was consistently (i.e., across subjects and hemispheres) more activated by one of our two GVS conditions.

Activations During Sham Stimulation

To confirm that the sham condition is a valid control for GVS somatosensory side effects, a group analysis ($n = 13$) of cortical activations during sham stimulation was performed (**Supplementary Figure S1**). Three clusters are observed in each hemisphere. Bilateral activation was found in V1 (Talairach space, −3, −75, 13 and 5, −73, 11 for left and right hemisphere, respectively) and fusiform gyrus (Talairach space, −27, −63, −7 and 26, −60, −9 for left and right hemisphere, respectively). Also, significant activation was found in the left primary somatosensory cortex (Talairach space, −56, −15, 13) and right middle occipital gyrus (Talairach space, 29, −77, 18) an area that has been involved in multisensory integration (Doehrmann et al., 2010; Renier et al., 2010). Interestingly, no significant activations were found in any of the ROIs used in this study.

Regions of Interest Analysis

We ran an ROI-based analysis to enable the comparisons between the responses from our different subjects (see the "Materials and Methods" section). Within all the ROIs (in both hemispheres) of our subjects, we computed the beta values corresponding to the AP GVS, Lat GVS, and the sham condition. These beta values were then corrected by subtracting the beta values of the baseline condition [see the "General Linear Model (GLM)" section]. **Figure 3** shows the results in all our ROIs (i.e., V6, VIP, CSv, hMT+, and PIC).

Responses in V6 were strongly dependent on the condition (rmANOVA, Greenhouse-Geisser corrected: $F_{(2)} = 32.02$, $p < 0.001$, $\eta^2 = 2.81$; **Figure 3**, **Table 2**). *Post hoc t*-tests confirmed that the beta values were significantly higher for the AP GVS condition ($t_{(9)} = 6.99$, $p < 0.0001$ when compared to the Lat condition and $t_{(9)} = 7.72$, $p < 0.0001$ when compared to the *sham* condition). We did not find any significant differences between the Lat condition and the *sham* condition ($t_{(9)} = 0.046$, $p = 0.964$). Responses were also strongly influenced by the condition in area VIP (rmANOVA, Greenhouse-Geisser corrected: $F_{(2)} = 5.52$, $p = 0.016$, $\eta^2 = 0.512$). In this ROI as well, *post hoc t*-tests showed that responses in the AP GVS condition were stronger than in the Lat condition ($t_{(9)} = 4.252$, $p < 0.05$). We did not find any significant differences between the Lat condition and the *sham* condition ($t_{(9)} = 0.667$, $p = 0.521$). Therefore, both areas V6 and VIP had specific responses during the antero-posterior GVS.

Responses in area CSv and hMT+ were both strongly modulated by condition (rmANOVA, Greenhouse-Geisser corrected: $F_{(2)} = 3.253$, $p < 0.001$, $\eta^2 = 3.59$ in CSv and $F_{(2)} = 4.522$, $p < 0.05$, $\eta^2 = 1.429$ in hMT+). In these ROIs, both the AP ($t_{(10)} = 4.22$, $p < 0.01$ in CSv and $t_{(9)} = 2.83$, $p = 0.05$ in hMT+) and Lat ($t_{(10)} = 4.24$, $p < 0.01$ in CSv and $t_{(9)} = 3.91$, $p = 0.05$ in hMT+) GVS conditions had stronger responses than the sham condition. This time, we did not find any significant difference between the two GVS conditions ($t_{(10)} = 1.03$, $p = 0.91$ in CSv and $t_{(9)} = -0.145$, $p = 0.887$ in hMT+).

Finally, responses in PIC were also dependent on the condition (rmANOVA, Greenhouse-Geisser corrected:

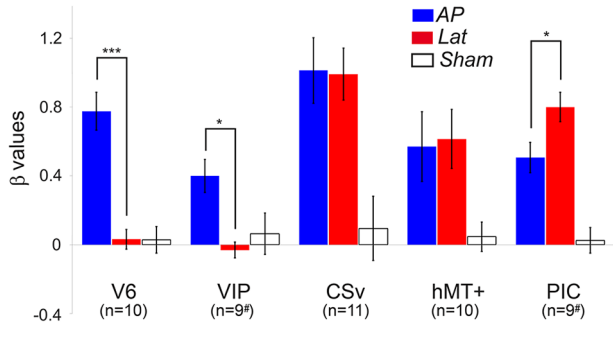

FIGURE 3 | Average beta values obtained in our different ROIs during the antero-posterior (blue) and lateral (red) GVS conditions. Values corresponding to the sham condition are provided in white. The error bars give the standard errors. The # symbols are here to remind that in some subjects, the ventral intraparietal (VIP) and posterior insular cortex (PIC) ROIs were only defined in one hemisphere (see details in the text). We report here the significant differences between AP and Lat conditions (*post hoc t*-test, ***$p < 0.001$, *$p < 0.05$). The results of the other statistical comparisons are reported in the main document.

TABLE 2 | Paired *t*-test results, contrasting beta-values obtained in antero-posterior (AP), lateral (LAT), and sham condition, for our five Regions of Interest (ROIs), by taking all (100%) voxels, and the 80% and 60% closest to the central coordinates.

100%			
AREA	**AP-LAT**	**AP-SHAM**	**LAT-SHAM**
V6	$t_{(9)} = 6.99$, $p = 0.000064$	$t_{(9)} = 7.72$, $p = 0.000029$	$t_{(9)} = 0.046$, $p = 0.964$
VIP	$t_{(9)} = 4.252$, $p = 0.021$	$t_{(9)} = 2.625$, $p = 0.029$	$t_{(9)} = 0.667$, $p = 0.521$
CSV	$t_{(10)} = 1.03$, $p = 0.91$	$t_{(10)} = 4.22$, $p = 0.002$	$t_{(10)} = 4.24$, $p = 0.02$
hMT+	$t_{(9)} = -0.145$, $p = 0.887$	$t_{(9)} = 2.83$, $p = 0.019$	$t_{(9)} = 3.91$, $p = 0.003$
PIC	$t_{(9)} = -2.41$, $p = 0.0269$	$t_{(9)} = 4.193$, $p = 0.002$	$t_{(9)} = 6.86$, $p = 0.000081$
80%			
V6	$t_{(9)} = 4.07$, $p = 0.003$	$t_{(9)} = 2.96$, $p = 0.016$	$t_{(9)} = 0.738$, $p = 0.479$
VIP	$t_{(9)} = 2.503$, $p = 0.034$	$t_{(9)} = 4.391$, $p = 0.002$	$t_{(9)} = 2.705$, $p = 0.026$
CSV	$t_{(10)} = 0.386$, $p = 0.708$	$t_{(10)} = 3.416$, $p = 0.007$	$t_{(10)} = 4.399$, $p = 0.001$
hMT+	$t_{(8)} = 0.247$, $p = 0.811$	$t_{(8)} = 4.04$, $p = 0.003$	$t_{(8)} = 5.012$, $p = 0.001$
PIC	$t_{(9)} = 2.705$, $p = 0.024$	$t_{(9)} = 4.256$, $p = 0.002$	$t_{(9)} = 6.36$, $p = 0.000131$
60%			
V6	$t_{(9)} = 2.822$, $p = 0.02$	$t_{(9)} = 2.545$, $p = 0.027$	$t_{(9)} = 1.101$, $p = 0.3$
VIP	$t_{(9)} = 2.872$, $p = 0.018$	$t_{(9)} = 4.923$, $p = 0.000821$	$t_{(9)} = 2.339$, $p = 0.044$
CSV	$t_{(10)} = 0.555$, $p = 0.592$	$t_{(10)} = 2.301$, $p = 0.04$	$t_{(10)} = 3.126$, $p = 0.011$
hMT+	$t_{(7)} = 0.073$, $p = 0.944$	$t_{(7)} = 3.346$, $p = 0.012$	$t_{(7)} = 3.394$, $p = 0.011$
PIC	$t_{(9)} = 0.187$, $p = 0.856$	$t_{(9)} = 4.574$, $p = 0.001$	$t_{(9)} = 6.254$, $p = 0.000149$

$F_{(2)} = 55.55$, $p < 0.001$, $\eta^2 = 1.579$). In this case, *post hoc* *t*-tests confirmed that responses were stronger during the Lat GVS condition than during the AP GVS condition ($t_{(9)} = -2.41$, $p < 0.05$). Responses during the AP and Lat conditions were stronger than during the *sham* condition ($t_{(9)} = 4.193$, $p < 0.01$ and $t_{(9)} = 6.86$, $p < 0.001$, respectively). As stated in the "Materials and Methods" section, we looked for activation in an additional ROI, PIVC, defined from former studies (Frank et al., 2016), to compare with PIC (**Supplementary Figure S2**). Given that the results are noisy, probably due to the ROI definition procedure, a one-sample *t*-test against 0 showed significant values for antero-posterior (AP): $t_{(12)} = 2.68$, $p = 0.02$ and for lateral (Lat): $t_{(12)} = 2.47$, $p = 0.03$ but not for Sham condition (Sham): $t_{(12)} = 0.57$, $p = 0.58$.

Among all our ROIs, CSv had the strongest responses to GVS conditions. This result is consistent with those reported in Smith et al. (2012). Overall, our results demonstrate that the activations elicited by Lat GVS in areas V6, VIP, CSv, hMT+, and PIC are reliable across different stimulation parameters (a 1 Hz sinewave alternating between ±3 mA in Smith et al., 2012 vs. a 1 mA step in the present study).

We observed in the "Region of Interest (ROI) Definition" section that our procedure to define area V6, which did not include wide-field retinotopic mapping, cannot guarantee that this ROI does not include small portions from adjacent areas in some subjects. To make sure that the effects reported here reflect properties of area V6, we performed a control analysis where we reproduced our statistics on subsamples of voxels within this ROI. We first computed the Euclidean distances between all the voxels within the ROI and the ROI center. We then defined two smaller ROIs that grouped either the 80 or the 60% of voxels that were the closest to the central coordinates. These smaller ROIs have less chance to contain voxels that do not belong to V6. As the ROI centers were not strictly identical for all the subjects, this process could exclude the subject for whom the cluster was outside from the reduced ROI, explaining why the number of subjects slightly decreases from 100% to 80 and 60%.

The results of this analysis are shown in **Figure 4** and **Table 2** reports all the paired *t*-test contrasts between the GVS conditions, for our five ROIs.

We can observe that our main results (**Figure 4**, **Table 2**) remained unchanged with this analysis. It demonstrates that the preference for AP GVS stimulation that we found in V6 is robust to variation in the spatial extent used to define this area and, therefore, not driven by activity within adjacent functional areas. We used the same approach to double-check our results in the VIP, CSv, hMT+, and PIC ROIs. Indeed, these areas were defined from thresholded contrast maps ($p < 0.001$, uncorrected, see the "Materials and Methods" section), which is always subject to uncertainty, see e.g., Eickhoff et al. (2009). This control analysis confirmed our results in areas CSv, hMT+, and VIP. In particular, for area VIP, it demonstrated that the preference for AP GVS did not depend on the spatial extent used to define this ROI. Interestingly, our control confirmed that responses in PIC during Lat GVS were stronger than during AP GVS only for the 80% of voxels but not for the 60% ($t_{(9)} = 2.705$, $p = 0.024$ and $t_{(9)} = 0.187$, $p = 0.856$, respectively). This result should, therefore, be taken with care and will probably necessitate further investigations.

Connectivity Analysis

The differential activation within our visual ROIs during antero-posterior (AP) and lateral (lat) conditions support the hypothesis that antero-posterior and lateral vestibular signals are processed by distinct cortical networks. Nevertheless, it does not provide any information regarding interactions between these areas and the structure of these networks. To identify the connectivity pattern between our functionally defined ROIs, we ran a *multiregional PPI* analysis (see the "Connectivity Analysis" section). For this type of analysis, all ROIs must be defined in each subject. It was, therefore, only performed on the nine subjects for whom all the ROIs were defined. If V6 and VIP are more activated during the AP compatible

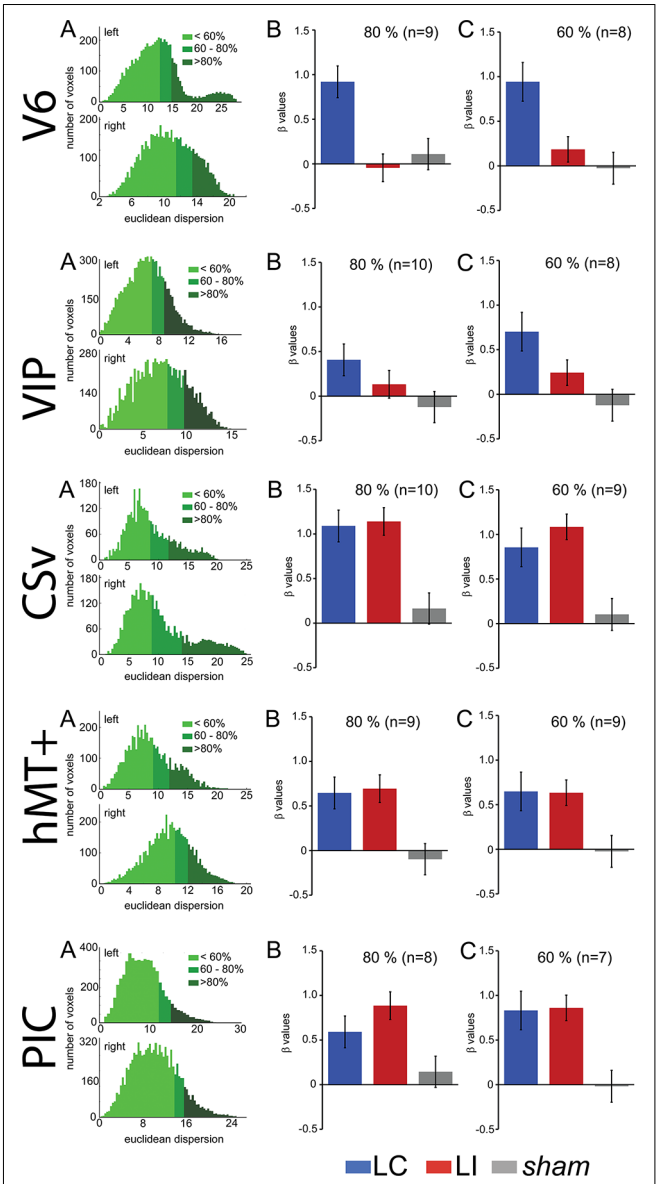

FIGURE 4 | Control to characterize the influence of the ROI spatial extents on the results. These analyses were performed for V6, cingulate sulcus visual (CSv), hMT+, VIP, and PIC (from top to bottom). **(A)** Histograms showing the number of voxels within an ROI as a function of the Euclidean distance to the ROI centroid. The green colors give the repartition of 60%, 80%, and 100% closest voxels. **(B)** Bar graphs of the beta values for the two GVS conditions (AP, in blue and Lat, in red) and the sham stimulation. The analysis only included the 80% closest voxels to the centroid. **(C)** Idem for the 60% closest voxels.

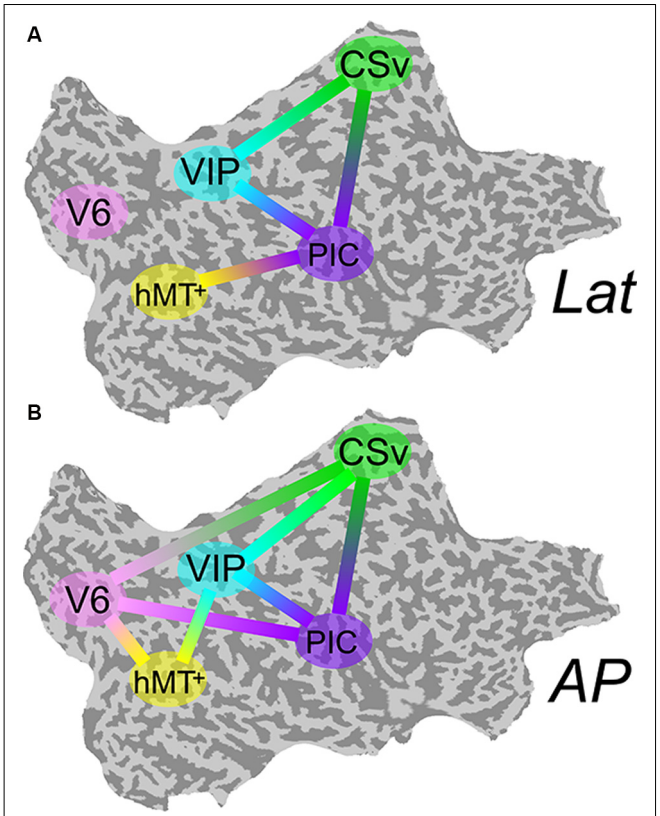

FIGURE 5 | Psychophysiological interaction (PPI) functional connectivity analysis. Multiregional PPI was run across the five ROIs identified in the localizer protocol. Results are shown for the Lat **(A)** and AP **(B)** GVS conditions. A solid line between two ROIs corresponds to a connection that is significantly stronger during this condition ($P < 0.001$) than during baseline.

condition, one could expect that connectivity between each of these ROIs and the others are more pronounced during this condition. **Figure 5A** shows connections between our ROIs that are significantly more correlated during the lat condition than during baseline. **Figure 5B** shows these correlations for the AP condition.

During Lat GVS, areas PIC, hMT+, CSv, and VIP were more connected than during baseline (5-A). This was particularly true for area PIC. The connectivity pattern between V6 and the other ROIs remained at the baseline level for this condition. At the opposite, during AP GVS, V6 was significantly more connected to CSv, hMT+, and PIC (5-B) than during baseline ($P < 0.001$). Area VIP was also significantly more connected to hMT+ during this condition ($P < 0.001$), whereas it was not the case during the Lat condition.

To determine if cortical activations were different in the subjects who detected the GVS direction over chance, we looked for a correlation between behavior outcome (d' sensitivity) and brain activity. We did not find any significant relationship between our fMRI measurements and our subject's perceptual reports. This was true for both the beta values of each region and the connectivity strengths (and amount of connected pairs). Given the low intensity used in our design, and above all the too short stimulation duration to allow the building of conscious vection, it is possible that the elicited percept was not strong enough or that the limited amount of subjects does not allow to uncover a small effect to establish such correlations.

Control for Vergence

Our results showed that areas V6 and VIP are only activated during antero-posterior GVS. One possibility is that, even if our participants had their eyes closed, this condition triggered

convergence or divergence eye movement and these movements affected the activity in V6 and/or VIP. For example, a study by Quinlan and Culham (2007) showed that responses in the dorsal POS (dPOS, a brain portion that includes V6) were modulated by the vergence angle. To control that GVS (and specifically the stimulations associated with a backward or forward motion of the body) did not trigger convergence and/or divergence movement of the two eyes, we performed a control experiment outside of the scanner. For this control, subjects had their eyes opened and binocularly viewed Nonius lines (see Cottereau et al., 2011) through anaglyph goggles with red/green filter on the left/right eye. The green line was displayed in the upper part of the visual field and was only seen by the right eye (through the green filter). The red line was displayed in the bottom part of the visual field and was only seen by the left eye (through the red filter). The two lines were vertically aligned with a visible fixation point at the center of the screen. When binocularly viewed through the anaglyph goggles, this configuration appeared as two white lines vertically aligned with a white dot on the center of the screen. The subject task was to fixate the point during blocks of GVS that were identical to those used in our main experiment (see the "Materials and Methods" section). After each stimulation, subjects had to report if they perceived the two lines as "aligned" during GVS (upper arrow of the keyboard) or if the upper line moved to the left (left arrow) or the right (right arrow) relatively to the bottom line. These last two cases, respectively, correspond to convergence and divergence eye movements. The sensitivity to Nonius misalignment is typically below 2 arcmin (McKee and Levi, 1987), which is more accurate than what can be obtained from a binocular eye tracker. Five subjects who participated in the galvanic stimulation experiment performed 20 trials of each condition. Their perceptual reports are provided in **Figure 6**.

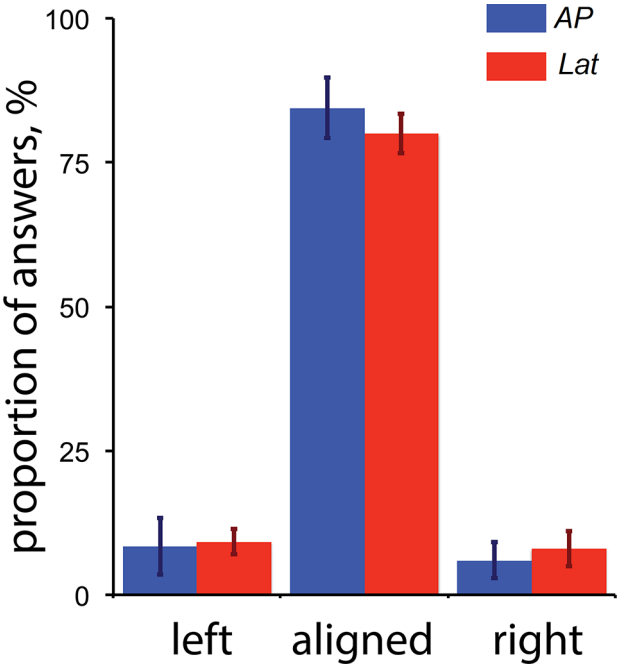

FIGURE 6 | Perceptual reports during the control experiment for vergence (n = 5). The proportion of "left," "aligned" and "right" answers are provided for both the antero-posterior (AP) and lateral (Lat) conditions. The "left" and "right" reports respectively correspond to convergence and divergence eye movements (see details in the text). The error bars give the standard errors.

These results demonstrate that: (1) GVS had a minor impact on binocular eye movements; and (2) the small proportions of reported convergence/divergence movements were not statistically different between our AP and Lat GVS conditions. We conclude that the activations elicited by our AP condition in V6 were not caused by eye movements.

Even though our subjects had their eyes closed during the fMRI recordings, we cannot exclude that their lateral eye movements were different between our two conditions. If it is a limitation of our study, we are confident that our results are not contaminated by lateral eye movements. Indeed, our analyses were performed in functional ROIs that are not specifically known to respond to lateral eye movements. Also, our whole-brain analysis did not reveal any significant activation in regions whose responses are modulated by lateral eye movements like for example the frontal eye field.

DISCUSSION

This study aimed to characterize the cortical networks that are activated during antero-posterior (AP) and lateral (Lat) GVS using fMRI measurements. A previous neuroimaging study employed the usual binaural bipolar mode, where the anode is placed on one mastoid process and the cathode on the other to identify visual cortical areas that receive vestibular inputs (Smith et al., 2012). In the present study, we applied lateral GVS using an opposite double monaural configuration (see **Figure 1B**) that was found to induce equivalent postural response than binaural bipolar (Séverac Cauquil et al., 2000). Recent electrophysiology studies using GVS on macaque monkeys showed that anodal and cathodal have the opposite effect on vestibular afferents discharge of both otolith and semicircular canals (Kwan et al., 2019). This corroborates the assumption that the orientation of the response to GVS is a function of the imbalance between right and left vestibular polarization (Séverac Cauquil et al., 2000). Here, we replicated Smith's results obtained from 3 mA sinusoidal binaural bipolar stimulation using a 1 mA step pulse in opposite double monaural GVS, validating the robustness of the GVS approach. However, such lateral GVS configurations activate the parts of the vestibular apparatus that are sensitive to roll tilt, in the frontal plane (Day et al., 1997; Séverac Cauquil et al., 2003; Fitzpatrick and Day, 2004). Therefore, this design prohibits the study of the consequences of an antero-posterior stimulation, although these signals are the most prominent during locomotion, which constitutes a major component of egomotion. We, therefore, used binaural monopolar GVS to investigate the cortical responses specific to antero-posterior mechanisms. This design, with electrodes of the same polarity placed over the mastoid processes, and of opposite polarity on the forehead orientates the galvanic-evoked vestibular input along the antero-posterior axis (Séverac

Cauquil et al., 1998, 2000; Magnusson et al., 1990; Aoyama et al., 2015; see **Figure 1**). This permitted us to distinguish the contribution of AP signals from the Lat ones provided by the usual, binaural bipolar mode. Our behavioral analysis supports those previously reported results. Even though our subjects were lying in the scanner, 7 over 13 were still able to discriminate over chance the stimulated direction of self-motion. Regarding the low intensity (1 mA vs. 3 mA in Aoyama et al., 2015) and short duration (2 s vs. 5 s in report Fitzpatrick et al., 2002) and taking into account the fact that here we submitted our subjects to a discrimination and not a detection task, we are entitled to consider we achieved to stimulate in two different directions our subjects' vestibular apparatuses.

As a preliminary step, we performed for each subject a whole-brain analysis to get a general overview of our data. Across the subject, our two GVS conditions led to strong fMRI activations within lateral sulcus, in the PIVC. This, corroborated by the introduction of PIVC as a supplementary ROI based on published coordinates, is in agreement with previous studies that found significant activations in the same region (Bucher et al., 1998; Lobel et al., 1998; Bense et al., 2001; Stephan et al., 2005) and with a recent hypothesis suggesting that PIVC is a complex that contains visual and non-visual areas specialized in different functions (Frank and Greenlee, 2018). However, we were mostly interested in responses within functionally defined ROIs that are activated by egomotion-consistent optic flow: V6, VIP, CSv, hMT+, and PIC (see Cardin and Smith, 2010; **Figure 2**). Our aim was to better understand how these visual ROIs process vestibular inputs and hence their possible implication in multisensory integration during forward locomotion.

We found that area PIC was significantly activated during both our two GVS conditions (**Figure 3**). This result is in agreement with a previous multisensory study (Frank et al., 2014). Our connectivity analysis showed that PIC is the most connected area during galvanic stimulation (**Figure 5**). This area possibly works as a hub where multisensory signals are integrated during egomotion. This strong selectivity to both visual and vestibular modalities supports the idea that PIC is the human homolog of macaque visual posterior Sylvian area (VPS; Chen et al., 2011). This is in total agreement with previous single-unit recordings and tracer studies in non-human primates (Guldin and Grüsser, 1998). In the macaque, this portion of cortex receives inputs from all the cortical areas of the vestibular system and also, even more, relevant for our study, its neurons are sensitive to both somatosensory and visual signals, in particular to optokinetic stimulation from wide (i.e., $>30°$) structured patterns (Grüsser et al., 1990). Even though defined from former studies (Frank et al., 2016) rather than localizers, we had a look at PIVC activation which is noisier, probably due to the definition procedure, not different between Lat and AP, and twice as smaller as PIC (**Supplementary Figure S2**).

A major finding of this study is that area V6 is only activated during antero-posterior GVS (**Figure 3**). Using lateral GVS, a previous study (Smith et al., 2012) did not find any activation in V6 and concluded that this area was probably not involved in visuo-vestibular integration. Our results are in agreement with the finding that V6 remains silent during lateral stimulation. However, the strong responses that we obtained during AP GVS show that V6 does receive vestibular input and has probably a specific role during locomotion. This hypothesis is strengthened by our PPI analyses that demonstrated that area V6 becomes significantly more connected to all our other ROIs during AP GVS (**Figure 5**). A recent study showed that there is another visual region bordering V6: V6A (Pitzalis et al., 2013). This area is mostly responsive to peripheral representation ($\geq 30°$) and lacks the central part of the visual field. Our optic flow stimulus spanned a square of $16° \times 16°$ and it is, therefore, likely that it activated V6 and not V6A. Future studies should however include a wide field retinotopic mapping in their procedures to delineate these two regions. A previous fMRI study in humans found that responses in the dorsal POS (dPOS, a region that includes V6) were modulated by the vergence angle (Quinlan and Culham, 2007). Our control experiment (see the "Control for Vergence" section) ruled out the possibility that our results are affected by vergence. In human, V6 responds to 3D translational egomotion (Sdoia et al., 2009). Its responses to optic flow are also enhanced when the flow is combined with congruent binocular disparity values (Cardin et al., 2012a). These observations and our results suggest that V6 might have a specific role during locomotion. In the macaque, V6 is often described as a principally visual area. A tracer study showed that anatomically, it is mostly connected to other visual regions, including areas MST and VIP (Galletti et al., 2001). Its responses are strongly influenced by optic flow signals but are not modulated by inertial motion (Fan et al., 2015). If areas V6 in human and macaque share similar visual properties, like their retinotopic organization (Pitzalis et al., 2006, 2012) or their selectivity to optic flow (Cardin and Smith, 2010; Fan et al., 2015; but see Cottereau et al., 2017), our results suggest that human V6 has a specific role for processing locomotion consistent vestibular inputs. It is, therefore, possible that the homology between human and macaque V6 is not as pronounced as currently believed (Pitzalis et al., 2013, 2015).

Our results also suggest an implication of area VIP in the processing of vestibular inputs. Responses to Lat GVS in this area did not differ from those measured during the sham condition. In their study, Smith et al. (2012) also reported that Lat GVS did not elicit significant responses in this area. However, our PPI estimation demonstrated that connections between VIP and areas CSv and PIC were significantly stronger during Lat GVS than during baseline (**Figure 5A**). The results of this connectivity analysis suggest that area VIP might be implicated in the processing of Lat GVS even though further investigation is needed to better understand its exact role in this condition. VIP responses were significantly stronger during AP GVS (**Figure 3**) and VIP was also more connected to the other ROIs during this condition (see the additional connection to hMT+ in **Figure 5B**). VIP is, therefore, involved during AP GVS and could be included in a cortical network processing vestibular signals, with a strong preference for the antero-posterior direction. In human, VIP is activated by different depth cues such as egomotion compatible

optic flow (Wall and Smith, 2008), and disparity (Yang et al., 2011). This area is the putative homologous of macaque VIP, see e.g., Bremmer et al. (2001), a multisensory area that integrates visual and vestibular inputs (Bremmer et al., 2002; Schlack et al., 2002; Chen et al., 2011). In particular, VIP in macaque strongly responds to optic flow (Cottereau et al., 2017) and is supposed to play an important role in navigation in space (Bremmer, 2005). Altogether, these results are in line with our findings and suggest that area VIP is important for locomotion in both human and macaque.

Significant activations were found in both hMT+ and CSv during AP and Lat GVS conditions. For lateral stimulation, our results are consistent with those of Smith et al. (2012). This study found that CSv had the strongest responses to this condition. This is also the case in our results (see **Figure 3**). Smith et al. (2012) also found that MST but not MT was activated during lateral GVS. In our study, we did not perform the localizers that permit to dissociate between MT and MST and we, therefore, only localized the human middle temporal complex (i.e., hMT+) using a functional localizer based on optic flow (see the "Materials and Methods" section). The hMT+ complex includes both MT and MST, and might also contain other regions such as the putative homologs of macaque areas FST and V4t (see Kolster et al., 2010). In our data, we did not find any significant difference between the responses to AP vs. Lat GVS in both CSv and hMT+. This suggests that the global responses of these areas are equivalent to our two GVS conditions. Note, however, that this does not rule out the possibility that subregions within CSv and/or hMT+ are selective to either one or the other condition. This distinction remains difficult to make at the macroscopic level of fMRI recordings and will need further investigations.

DATA AVAILABILITY STATEMENT

The datasets generated for this study are available on request to the corresponding author.

ETHICS STATEMENT

Ethics committee that approved the study: Comité de Protection des Personnes Sud Ouest et Outre Mer II (CPPSOOM II). Consent procedure used for participants: pre-included subjects were given an information note describing the experiment and gave their informed consent using a consent form. Both the information note and the consent form were approved by the CPPSOOM II.

AUTHOR CONTRIBUTIONS

AS, SC, and FA-J contributed to the conception and design of the study and data recording. The experiments and analyses were conceptualized by all the authors. Data analysis was performed by FA-J with substantial input from BC. All authors were involved in writing the manuscript. FA-J is now at the Institute of Pathophysiology, Johannes Gutenberg University of Mainz.

FUNDING

This work was funded by a grant from the French national research agency (ANR 12-BSV4-0005-01-OPTIVISION). BC was funded by a Marie Curie grant (PIIF-GA-2011-298386 Real-Depth). The fMRI recordings were funded by a grant from the Institut des Sciences du Cerveau de Toulouse (ISCT).

ACKNOWLEDGMENTS

We would like to thank Maxime Rosito for the development of the galvanic stimulation system and its adaptation to the scanner environment. We thank the INSERM U825 MRI technical platform for the MRI acquisitions and Jean-Pierre Jaffrézou for his thorough revision of the English. This manuscript has been released as a Pre-Print at BioRxiv (Aedo-Jury et al., 2019).

SUPPLEMENTARY MATERIAL

The Supplementary Material for this article can be found online at: https://www.frontiersin.org/articles/10.3389/fnint.2020.00043/full#supplementary-material.

FIGURE S1 | Activations during sham stimulation: group analysis (n = 13) of cortical activations during sham stimulation. Bilateral activation was found in V1 (Talairach space, −3, −75, 13 and 5, −73, 11 for left and right hemisphere, respectively) and fusiform gyrus (Talairach space, −27, −63, −7 and 26, −60, −9 for left and right hemisphere, respectively). Also, significant activation was found in the left primary somatosensory cortex (Talairach space, −56, −15, 13) and right middle occipital gyrus (Talairach space, 29, −77, 18).

FIGURE S2 | Putative parieto-insular vestibular cortex (PIVC) is active during Lat and AP galvanic stimulation. **(A)** PIVC coordinates were taken from Frank et al. (2016), a sphere of 300 voxels was drawn around the center of Talairach coordinates (−43, −14, 17 and 40, −14, 18 for left and right hemisphere, respectively) and the beta values extracted for each subject from the normalized Talairach brain. The position of the sphere in the cortical flat map is purely illustrative. **(B)** Average beta values and standard errors obtained for PIVC in both hemispheres (n = 13) during the AP (blue) and Lat (red) GVS conditions. Values corresponding to the sham condition are provided in white. One sample t-test against 0 showed significant values for AP: $t_{(12)} = 2.68$, $p = 0.02$—and for Lat: $t_{(12)} = 2.47$, $p = 0.03$—but not for Sham condition (Sham): $t_{(12)} = 0.57$, $p = 0.58$.

REFERENCES

Aedo-Jury, F., Cottereau, B. R., Celebrini, S., and Severac Cauquil, A. (2019). Antero-posterior versus lateral vestibular input processing in human visual cortex. *BioRxive* [Preprint].doi: 10.1101/530808

Aoyama, K., Iizuka, H., Ando, H., and Maeda, T. (2015). Four-pole galvanic vestibular stimulation causes body sway about three axes. *Sci. Rep.* 5:10168. doi: 10.1038/srep10168

Bense, S., Stephan, T., Yousry, T. A., Brandt, T., and Dieterich, M. (2001). Multisensory cortical signal increases and decreases during vestibular galvanic stimulation (fMRI). *J. Neurophysiol.* 85, 886–899. doi: 10.1152/jn.2001.85.2.886

Billington, J., and Smith, A. T. (2015). Neural mechanisms for discounting head-roll-induced retinal motion. *J. Neurosci.* 35, 4851–4856. doi: 10.1523/JNEUROSCI.3640-14.2015

Bremmer, F. (2005). Navigation in space—the role of the macaque ventral intraparietal area. *J. Physiol.* 566, 29–35. doi: 10.1113/jphysiol.2005.082552

Bremmer, F., Klam, F., Duhamel, J. R., Ben Hamed, S., and Graf, W. (2002). Visual-vestibular interactive responses in the macaque ventral intraparietal area (VIP). *Eur. J. Neurosci.* 16, 1569–1586. doi: 10.1046/j.1460-9568.2002.02206.x

Bremmer, F., Kubischik, M., Pekel, M., Lappe, M., and Hoffmann, K. P. (1999). Linear vestibular self-motion signals in monkey medial superior temporal area. *Ann. N Y Acad. Sci.* 871, 272–281. doi: 10.1111/j.1749-6632.1999.tb09191.x

Bremmer, F., Schlack, A., Shah, N. J., Zafiris, O., Kubischik, M., Hoffmann, K., et al. (2001). Polymodal motion processing in posterior parietal and premotor cortex: a human fMRI study strongly implies equivalencies between humans and monkeys. *Neuron* 29, 287–296. doi: 10.1016/s0896-6273(01)00198-2

Britten, K. H. (2008). Mechanisms of self-motion perception. *Annu. Rev. Neurosci.* 31, 389–410. doi: 10.1146/annurev.neuro.29.051605.112953

Bucher, S. F., Dieterich, M., Wiesmann, M., Weiss, A., Zink, R., Yousry, T. A., et al. (1998). Cerebral functional magnetic resonance imaging of vestibular, auditory, and nociceptive areas during galvanic stimulation. *Ann. Neurol.* 44, 120–125. doi: 10.1002/ana.410440118

Cardin, V., Hemsworth, L., and Smith, A. T. (2012a). Adaptation to heading direction dissociates the roles of human MST and V6 in the processing of optic flow. *J. Neurophysiol.* 108, 794–801. doi: 10.1152/jn.00002.2012

Cardin, V., Sherrington, R., Hemsworth, L., and Smith, A. T. (2012b). Human V6: functional characterisation and localisation. *PLoS One* 7:e47685. doi: 10.1371/journal.pone.0047685

Cardin, V., and Smith, A. T. (2010). Sensitivity of human visual and vestibular cortical regions to egomotion-compatible visual stimulation. *Cereb. Cortex* 20, 1964–1973. doi: 10.1093/cercor/bhp268

Chen, A., DeAngelis, G. C., and Angelaki, D. E. (2011). Representation of vestibular and visual cues to self-motion in ventral intraparietal cortex. *J. Neurosci.* 31, 12036–12052. doi: 10.1523/JNEUROSCI.0395-11.2011

Cocchi, L., Halford, G. S., Zalesky, A., Harding, I. H., Ramm, B. J., Cutmore, T., et al. (2014). Complexity in relational processing predicts changes in functional brain network dynamics. *Cereb. Cortex* 24, 2283–2296. doi: 10.1093/cercor/bht075

Cottereau, B. R., McKee, S. P., Ales, J. M., and Norcia, A. M. (2011). Disparity-tuned population responses from human visual cortex. *J. Neurosci.* 31, 954–965. doi: 10.1523/JNEUROSCI.3795-10.2011

Cottereau, B. R., McKee, S. P., and Norcia, A. M. (2014). Dynamics and cortical distribution of neural responses to 2D and 3D motion in human. *J. Neurophysiol.* 111, 533–543. doi: 10.1152/jn.00549.2013

Cottereau, B. R., Smith, A. T., Rima, S., Fize, D., Héjja-Brichard, Y., Renaud, L., et al. (2017). Processing of egomotion-consistent optic flow in the rhesus macaque cortex. *Cereb. Cortex* 27, 330–343. doi: 10.1093/cercor/bhw412

Day, B. L., Ramsay, E., Welgampola, M. S., and Fitzpatrick, R. C. (2011). The human semicircular canal model of galvanic vestibular stimulation. *Exp. Brain Res.* 210, 561–568. doi: 10.1007/s00221-011-2565-7

Day, B. L., Séverac Cauquil, A., Bartolomei, L., Pastor, M. A., and Lyon, I. N. (1997). Human body-segment tilts induced by galvanic stimulation: a vestibularly driven balance protection mechanism. *J. Physiol.* 500, 661–672. doi: 10.1113/jphysiol.1997.sp022051

Doehrmann, O., Weigelt, S., Altmann, C. F., Kaiser, J., and Naumer, M. J. (2010). Audiovisual functional magnetic resonance imaging adaptation reveals multisensory integration effects in object-related sensory cortices. *J. Neurosci.* 30, 3370–3379. doi: 10.1523/JNEUROSCI.5074-09.2010

Duffy, C. J. (1998). MST neurons respond to optic flow and translational movement. *J. Neurophysiol.* 80, 1816–1827. doi: 10.1152/jn.1998.80.4.1816

Eickhoff, S. B., Laird, A. R., Grefkes, C., Wang, L. E., Zilles, K., and Fox, P. T. (2009). Coordinate-based activation likelihood estimation meta-analysis of neuroimaging data: a random-effects approach based on empirical estimates of spatial uncertainty. *Hum. Brain Mapp.* 30, 2907–2926. doi: 10.1002/hbm.20718

Fan, R. H., Liu, S., DeAngelis, G. C., and Angelaki, D. E. (2015). Heading tuning in macaque area V6. *J. Neurosci.* 35, 16303–16314. doi: 10.1523/JNEUROSCI.2903-15.2015

Ferrè, E. R., Longo, M., Fiori, F., and Haggard, P. (2013). Vestibular modulation of spatial perception. *Front. Hum. Neurosci.* 7:660. doi: 10.3389/fnhum.2013.00660

Fitzpatrick, R. C., and Day, B. L. (2004). Probing the human vestibular system with galvanic stimulation. *J. Appl. Physiol.* 96, 2301–2316. doi: 10.1152/japplphysiol.00008.2004

Fitzpatrick, R. C., Marsden, J., Lord, S. R., and Day, B. L. (2002). Galvanic vestibular stimulation evokes sensations of body rotation. *Neuroreport* 13, 2379–2383. doi: 10.1097/00001756-200212200-00001

Frank, S. M., Baumann, O., Mattingley, J. B., and Greenlee, M. W. (2014). Vestibular and visual responses in human posterior insular cortex. *J. Neurophysiol.* 112, 2481–2491. doi: 10.1152/jn.00078.2014

Frank, S. M., and Greenlee, M. W. (2018). The parieto-insular vestibular cortex in humans: more than a single area? *J. Neurophysiol.* 120, 1438–1450. doi: 10.1152/jn.00907.2017

Frank, S. M., Wirth, A. M., and Greenlee, M. W. (2016). Visual-vestibular processing in the human Sylvian fissure. *J. Neurophysiol.* 116, 263–271. doi: 10.1152/jn.00009.2016

Friston, K. J., Buechel, C., Fink, G. R., Morris, J., Rolls, E., and Dolan, R. J. (1997). Psychophysiological and modulatory interactions in neuroimaging. *NeuroImage* 6, 218–229. doi: 10.1006/nimg.1997.0291

Galletti, C., Gamberini, M., Kutz, D. F., Fattori, P., Luppino, G., and Matelli, M. (2001). The cortical connections of area V6: an occipito-parietal network processing visual information. *Eur. J. Neurosci.* 13, 1572–1588. doi: 10.1046/j.0953-816x.2001.01538.x

Gitelman, D. R., Penny, W. D., Ashburner, J., and Friston, K. J. (2003). Modeling regional and psychophysiologic interactions in fMRI: the importance of hemodynamic deconvolution. *NeuroImage* 19, 200–207. doi: 10.1016/s1053-8119(03)00058-2

Grüsser, O. J., Pause, M., and Schreiter, U. (1990). Vestibular neurones in the parieto-insular cortex of monkeys (Macaca fascicularis): visual and neck receptor responses. *J. Physiol.* 430, 559–583. doi: 10.1113/jphysiol.1990.sp018307

Gu, Y., Watkins, P. V., Angelaki, D. E., and DeAngelis, G. C. (2006). Visual and nonvisual contributions to three-dimensional heading selectivity in the medial superior temporal area. *J. Neurosci.* 26, 73–85. doi: 10.1523/JNEUROSCI.2356-05.2006

Guldin, W. O., and Grüsser, O. J. (1998). Is there a vestibular cortex? *Trends Neurosci.* 21, 254–259. doi: 10.1016/s0166-2236(97)01211-3

Hupé, J. M. (2015). Statistical inferences under the Null hypothesis: common mistakes and pitfalls in neuroimaging studies. *Front. Neurosci.* 9:18. doi: 10.3389/fnins.2015.00018

Klam, F., and Graf, W. (2003a). Vestibular signals of posterior parietal cortex neurons during active and passive head movements in macaque monkeys. *Ann. N Y Acad. Sci.* 1004, 271–282. doi: 10.1196/annals.1303.024

Klam, F., and Graf, W. (2003b). Vestibular response kinematics in posterior parietal cortex neurons of macaque monkeys. *Eur. J. Neurosci.* 18, 995–1010. doi: 10.1046/j.1460-9568.2003.02813.x

Kolster, H., Peeters, R., and Orban, G. A. (2010). The retinotopic organization of the human middle temporal area MT/V5 and its cortical neighbors. *J. Neurosci.* 30, 9801–9820. doi: 10.1523/JNEUROSCI.2069-10.2010

Kwan, A., Forbes, P. A., Mitchell, D. E., Blouin, J.-S., and Cullen, K. E. (2019). Neural substrates, dynamics and thresholds of galvanic vestibular stimulation in the behaving primate. *Nat. Commun.* 10:1904. doi: 10.1038/s41467-019-09738-1

Lepecq, J. C., De Waele, C., Mertz-Josse, S., Teyssèdre, C., Tran Ba Huy, P., Baudonnière, P. M., et al. (2006). Galvanic vestibular stimulation modifies vection paths in healthy subjects. *J. Neurophysiol.* 95, 3199–3207. doi: 10.1152/jn.00478.2005

Lobel, E., Kleine, J. F., Bihan, D. L., Leroy-Willig, A., and Berthoz, A. (1998). Functional MRI of galvanic vestibular stimulation. *J. Neurophysiol.* 80, 2699–2709. doi: 10.1152/jn.1998.80.5.2699

Lopez, C., Blanke, O., and Mast, F. W. (2012). The human vestibular cortex revealed by coordinate-based activation likehood estimation mata-analysis. *Neuroscience* 212, 159–179. doi: 10.1016/j.neuroscience.2012.03.028

Lund, S., and Broberg, C. (1983). Effects of different head positions on postural sway in man induced by a reproducible vestibular error signal. *Acta Physiol. Scand.* 117, 307–309. doi: 10.1111/j.1748-1716.1983.tb07212.x

Magnusson, M., Johansson, R., and Wiklund, J. (1990). Galvanically induced body sway in the anterior-posterior plane. *Acta Otolaryngol.* 110, 11–17. doi: 10.3109/00016489009122509

McKee, S. P., and Levi, D. M. (1987). Dichoptic hyperacuity: the precision of nonius alignment. *J. Opt. Soc. Am. A* 4, 1104–1108. doi: 10.1364/josaa.4.001104

Morrone, M. C., Tosetti, M., Montanaro, D., Fiorentini, A., Cioni, G., and Burr, D. C. (2000). A cortical area that responds specifically to optic flow, revealed by fMRI. *Nat. Neurosci.* 3, 1322–1328. doi: 10.1038/81860

Nashner, L. M., and Wolfson, P. (1974). Influence of head position and proprioceptive cues on short latency postural reflexes evoked by galvanic stimulation of the human labyrinth. *Brain Res.* 67, 255–268. doi: 10.1016/0006-8993(74)90276-5

Njiokiktjien, C., and Folkerts, J. F. (1971). Displacement of the body's centre of gravity at galvanic stimulation of the labyrinth. *Confin. Neurol.* 33, 46–54. doi: 10.1159/000103102

Oldfield, R. C. (1971). The assessment and analysis of handedness: the Edinburgh inventory. *Neuropsychologia* 9, 97–113. doi: 10.1016/0028-3932(71)90067-4

O'Reilly, J. X., Woolrich, M. W., Behrens, T. E., Smith, S. M., and Johansen-Berg, H. (2012). Tools of the trade: psychophysiological interactions and functional connectivity. *Soc. Cogn. Affect. Neurosci.* 7, 604–609. doi: 10.1093/scan/nss055

Pitzalis, S., Fattori, P., and Galletti, C. (2012). The functional role of the medial motion area V6. *Front. Behav. Neurosci.* 6:91. doi: 10.3389/fnbeh.2012.00091

Pitzalis, S., Fattori, P., and Galletti, C. (2015). The human cortical areas V6 and V6A. *Vis. Neurosci.* 32:E007. doi: 10.1017/s0952523815000048

Pitzalis, S., Galletti, C., Huang, R. S., Patria, F., Committeri, G., Galati, G., et al. (2006). Wide-field retinotopy defines human cortical visual area v6. *J. Neurosci.* 26, 7962–7973. doi: 10.1523/JNEUROSCI.0178-06.2006

Pitzalis, S., Sereno, M. I., Committeri, G., Fattori, P., Galati, G., Tosoni, A., et al. (2013). The human homologue of macaque area V6A. *NeuroImage* 82, 517–530. doi: 10.1016/j.neuroimage.2013.06.026

Poldrack, R. A. (2007). Region of interest analysis for fMRI. *Soc. Cogn. Affect. Neurosci.* 2, 67–70. doi: 10.1093/scan/nsm006

Pozzo, T., Berthoz, A., and Lefort, L. (1990). Head stabilization during various locomotor tasks in humans—I. Normal subjects. *Exp. Brain Res.* 82, 97–106. doi: 10.1007/bf00230842

Quinlan, D. J., and Culham, J. C. (2007). fMRI reveals a preference for near viewing in the human parieto-occipital cortex. *NeuroImage* 36, 167–187. doi: 10.1016/j.neuroimage.2007.02.029

Renier, L. A., Anurova, I., De Volder, A. G., Carlson, S., VanMeter, J., and Rauschecker, J. P. (2010). Preserved functional specialization for spatial processing in the middle occipital gyrus of the early blind. *Neuron* 68, 138–148. doi: 10.1016/j.neuron.2010.09.021

Schindler, A., and Bartels, A. (2017). Connectivity reveals sources of predictive coding signals in early visual cortex during processing of visual optic flow. *Cereb. Cortex* 27, 2885–2893. doi: 10.1093/cercor/bhw136

Schlack, A., Hoffmann, K. P., and Bremmer, F. (2002). Interaction of linear vestibular and visual stimulation in the macaque ventral intraparietal area (VIP). *Eur. J. Neurosci.* 16, 1877–1886. doi: 10.1046/j.1460-9568.2002.02251.x

Sdoia, S., Pitzalis, S., Bultrini, A., Di Russo, F., Fattori, P., Galati, G., et al. (2009). Sensitivity to optic flow components in human cortical area V6 and other cortical motion areas. *NeuroImage* 47:S86. doi: 10.1016/s1053-8119(09)70645-7

Séverac Cauquil, A., Faldon, M., Popov, K., Day, B. L., and Bronstein, A. M. (2003). Short-latency eye movements evoked by near-threshold galvanic vestibular stimulation. *Exp. Brain Res.* 148, 414–418. doi: 10.1007/s00221-002-1326-z

Séverac Cauquil, A., Gervet, M. F., and Ouaknine, M. (1998). Body response to binaural monopolar galvanic vestibular stimulation in humans. *Neurosci. Lett.* 245, 37–40. doi: 10.1016/s0304-3940(98)00161-x

Séverac Cauquil, A., Martinez, P., Ouaknine, M., and Tardy-Gervet, M. F. (2000). Orientation of the body response to galvanic stimulation as a function of the inter-vestibular imbalance. *Exp. Brain Res.* 133, 501–505. doi: 10.1007/s002210000434

Smith, A. T., Wall, M. B., and Thilo, K. V. (2012). Vestibular inputs to human motion-sensitive visual cortex. *Cereb. Cortex* 22, 1068–1077. doi: 10.1093/cercor/bhr179

St George, R. J., Day, B. L., and Fitzpatrick, R. C. (2011). Adaptation of vestibular signals for self-motion perception. *J. Physiol.* 589, 843–853. doi: 10.1113/jphysiol.2010.197053

Stephan, T., Deutschländer, A., Nolte, A., Schneider, E., Wiesmann, M., Brandt, T., et al. (2005). Functional MRI of galvanic vestibular stimulation with alternating currents at different frequencies. *NeuroImage* 26, 721–732. doi: 10.1016/j.neuroimage.2005.02.049

Sunaert, S., Van Hecke, P., Marchal, G., and Orban, G. A. (1999). Motion-responsive regions of the human brain. *Exp. Brain Res.* 127, 355–370. doi: 10.1007/s002210050804

Talairach, J., and Tournoux, P. (1988). *Co-Planar Stereotaxic Atlas of the Human Brain: 3-Dimensional Proportional System—an Approach to Cerebral Imaging.* New York, NY: Thieme Medical Publishers, Inc.

Wall, M. B., and Smith, A. T. (2008). The representation of egomotion in the human brain. *Curr. Biol.* 18, 191–194. doi: 10.1016/j.cub.2007.12.053

Yang, Y., Liu, S., Chowdhury, S. A., DeAngelis, G. C., and Angelaki, D. E. (2011). Binocular disparity tuning and visual-vestibular congruency of multisensory neurons in macaque parietal cortex. *J. Neurosci.* 31, 17905–17916. doi: 10.1523/JNEUROSCI.4032-11.2011

Conflict of Interest: The authors declare that the research was conducted in the absence of any commercial or financial relationships that could be construed as a potential conflict of interest.